



This is a repository copy of *Structural investigation into the threading intercalation of a chiral dinuclear ruthenium(II) polypyridyl complex through a B-DNA oligonucleotide.*

White Rose Research Online URL for this paper:  
<http://eprints.whiterose.ac.uk/144384/>

Version: Supplemental Material

---

**Article:**

Fairbanks, S.D. [orcid.org/0000-0002-5063-1367](https://orcid.org/0000-0002-5063-1367), Robertson, C.C., Keene, F.R. [orcid.org/0000-0001-7759-0465](https://orcid.org/0000-0001-7759-0465) et al. (2 more authors) (2019) Structural investigation into the threading intercalation of a chiral dinuclear ruthenium(II) polypyridyl complex through a B-DNA oligonucleotide. *Journal of the American Chemical Society*, 141 (11). pp. 4644-4652. ISSN 0002-7863

<https://doi.org/10.1021/jacs.8b12280>

---

This document is the Accepted Manuscript version of a Published Work that appeared in final form in *Journal of the American Chemical Society*, copyright © American Chemical Society after peer review and technical editing by the publisher. To access the final edited and published work see: <https://doi.org/10.1021/jacs.8b12280>

**Reuse**

Items deposited in White Rose Research Online are protected by copyright, with all rights reserved unless indicated otherwise. They may be downloaded and/or printed for private study, or other acts as permitted by national copyright laws. The publisher or other rights holders may allow further reproduction and re-use of the full text version. This is indicated by the licence information on the White Rose Research Online record for the item.

**Takedown**

If you consider content in White Rose Research Online to be in breach of UK law, please notify us by emailing [eprints@whiterose.ac.uk](mailto:eprints@whiterose.ac.uk) including the URL of the record and the reason for the withdrawal request.



[eprints@whiterose.ac.uk](mailto:eprints@whiterose.ac.uk)  
<https://eprints.whiterose.ac.uk/>

## Structural investigation into the threading intercalation of a chiral dinuclear ruthenium (II) polypyridyl complex through a B-DNA oligonucleotide

Simon D. Fairbanks,<sup>†‡</sup> Craig C. Robertson,<sup>†</sup> F. Richard Keene,<sup>§</sup> Jim A. Thomas<sup>†\*</sup> and Mike P. Williamson<sup>†\*</sup>

<sup>†</sup>Department of Chemistry, University of Sheffield, Brook Hill, Sheffield, S3 7HF, UK.

Email: james.thomas@sheffield.ac.uk; Fax: +44-(0)114-22-29436

<sup>‡</sup>Department of Molecular Biology and Biotechnology, University of Sheffield, Western Bank, Sheffield, S10 2TN, UK. Email: m.williamson@sheffield.ac.uk.

<sup>§</sup>Department of Chemistry, School of Physical Sciences, University of Adelaide, Adelaide, SA 5005, Australia.

Page	contents
S2	SI 1; Figures S1-S3: crystallographic details
S6	SI 2; Figure S4: Induced CD for DNA plus <b>1</b> stereoisomers
S7	SI 3; Figure S5: Luminescence decay curves for <b>1</b> bound to oligonucleotide
S8	SI 4; Figure S6: NOE walk for free oligonucleotide
S9	SI 5; Figure S7: NMR assignments of the free Ru complexes
S9	SI 6; Table S1: NMR assignments for free and bound nucleotides
S11	SI 7; Table S2: Chemical shift values for Ru complexes, and shift changes on binding to DNA
S11	SI 8; Table S3, Figures S8-S10: Intermolecular NOEs
S14	SI 9; Figure S11: TOCSY spectra of TMe signals in $\Lambda,\Delta$ - <b>1</b> , free and bound to DNA
S14	SI 10; Figures S12-S14: EXSY spectra of thymidine methyls at 298 K, and fitting to obtain thermodynamic and kinetic parameters
S16	SI 11; Figure S15: <sup>31</sup> P COSY spectra of d- $\Lambda,\Delta$ - <b>1</b> and d- $\Lambda,\Lambda$ - <b>1</b> complexes
S17	SI 12; Figure S16: Spacefilling views of two alternative forms of the $\Lambda,\Delta$ - <b>1</b> complex
S17	references

## SI 1

A summary of crystallographic data and structure refinement of  $\Lambda, \Delta$ -1  $4(\text{Cl}) \cdot [(\text{bpy})_2\text{Ru}(\text{tpphz})\text{Ru}(\text{bpy})_2]^{4+}$

Identification code	iaj646k_0m
Empirical formula	$\text{C}_{64}\text{H}_{44}\text{Cl}_4\text{N}_{14}\text{Ru}_2$
Formula weight	1353.07
Temperature / K	100
Crystal system	Triclinic
Space group	P-1
a / Å	8.3032(16)
b / Å	11.378(2)
c / Å	18.250(4)
$\alpha$ / °	95.542(7)
$\beta$ / °	92.729(7)
$\gamma$ / °	95.095(7)
Volume / Å <sup>3</sup>	1706.6(6)
Z	1
$\rho_{\text{calc}}$ / gcm <sup>-3</sup>	1.317
$\mu$ / mm <sup>-1</sup>	0.646
F(000)	682.0
Crystal size / mm <sup>3</sup>	0.4 × 0.212 × 0.188
Radiation	MoK $\alpha$ ( $\lambda$ = 0.71073)
2 $\theta$ Range for Data Collection / °	3.612 to 55.112
Index Ranges	-10 ≤ h ≤ 10, -14 ≤ k ≤ 14, -23 ≤ l ≤ 23
Reflections Collected	46946
Independent Reflections	7843 [ $R_{\text{int}}$ = 0.0683, $R_{\text{sigma}}$ = 0.0575]
Data / Restraints / Parameters	7843/381/389
Goodness-of-fit on F <sup>2</sup>	1.022
Final R indexes [ $I \geq 2\sigma(I)$ ]	$R_1 = 0.0492$ , $wR_2 = 0.1183$
Final R indexes [all data]	$R_1 = 0.0707$ , $wR_2 = 0.1296$
Largest diff. peak/hole / e Å <sup>-3</sup>	1.84/-0.68

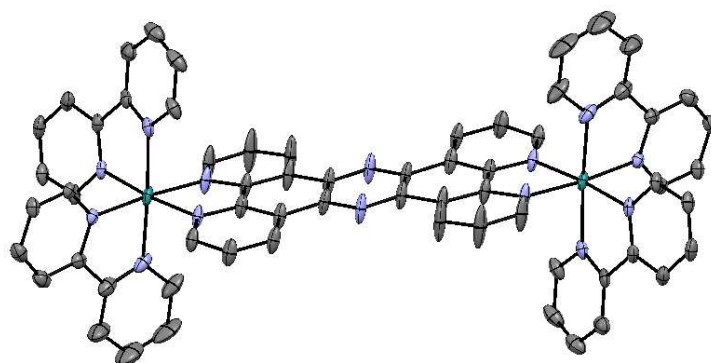


**Figure S1.** ORTEP plot of the X-ray crystallographic structure of  $\Lambda, \Delta$ -1 with thermal ellipsoids indicating 50% probability. Counter ions and solvent molecules omitted for clarity.

A summary of crystallographic data and structure refinement of  $\Lambda, \Lambda$ -1  $4[\text{PF}_6]^- \cdot [(\text{bpy})_2\text{Ru}(\text{tpphz})\text{Ru}(\text{bpy})_2]^{4+}$

Identification code	IJ674k_2_0m
Empirical formula	$\text{C}_{66}\text{H}_{50}\text{F}_{24}\text{N}_{16}\text{O}_4\text{P}_4\text{RU}_2$
Formula weight	1913.24
Temperature / K	100
Crystal system	Monoclinic
Space group	$P2_1$
a / Å	12.4658(7)
b / Å	16.2947(9)
c / Å	21.7440(12)
$\alpha$ / °	90
$\beta$ / °	97.257(3)
$\gamma$ / °	90
Volume / Å <sup>3</sup>	4381.4(4)
Z	2
$\rho_{\text{calc}} / \text{gcm}^{-3}$	1.450
$\mu / \text{mm}^{-1}$	0.520
F(000)	1908.0
Crystal size / mm <sup>3</sup>	0.5 × 0.2 × 0.18
Radiation	MoK $\alpha$ ( $\lambda = 0.71073$ )
2 $\theta$ Range for Data Collection / °	3.132 to 55.274
Index Ranges	$-16 \leq h \leq 16, -21 \leq k \leq 21, -28 \leq l \leq 28$
Reflections Collected	132518
Independent Reflections	20322 [ $R_{\text{int}} = 0.0879, R_{\text{sigma}} = 0.0750$ ]
Data / Restraints / Parameters	20322/1190/1105
Goodness-of-fit on F <sup>2</sup>	1.030
Final R indexes [ $ I  \geq 2\sigma(I)$ ]	$R_1 = 0.0710, wR_2 = 0.1735$
Final R indexes [all data]	$R_1 = 0.1063, wR_2 = 0.1925$
Largest diff. peak/hole / e Å <sup>-3</sup>	2.38/-0.80
Flack Parameter	0.065(9)

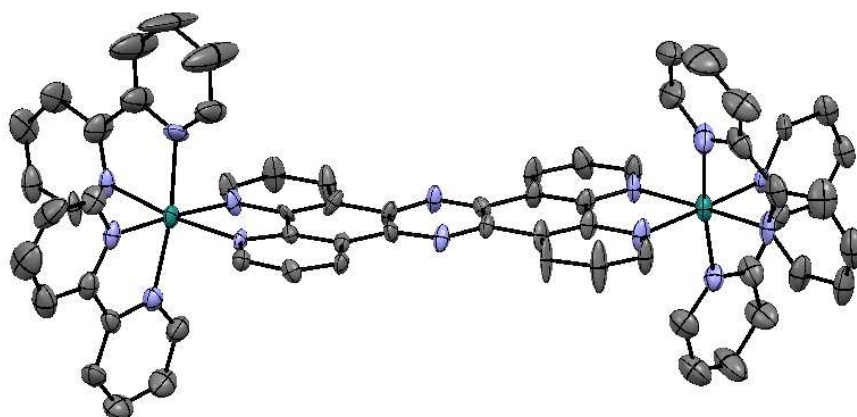


**Figure S2.** ORTEP plot of the X-ray crystallographic structure of  $\Lambda, \Lambda$ -1 with thermal ellipsoids indicating 50% probability. Counter ions and solvent molecules omitted for clarity.

A summary of crystallographic data and structure refinement of  $\Delta,\Delta$ -1  $4(\text{PF}_6)^- \cdot [(\text{bpy})_2\text{Ru}(\text{tpphz})\text{Ru}(\text{bpy})_2]^{4+}$

Identification code	IAJ672k_0m
Empirical formula	$\text{C}_{32}\text{H}_{22}\text{F}_{12}\text{N}_7\text{P}_2\text{Ru}$
Formula weight	895.57
Temperature / K	100
Crystal system	Monoclinic
Space group	$\text{P2}_1$
a / Å	12.5327(14)
b / Å	16.3645(19)
c / Å	21.809(3)
$\alpha$ / °	90
$\beta$ / °	97.129(5)
$\gamma$ / °	90
Volume / Å <sup>3</sup>	4438.3(9)
Z	4
$\rho_{\text{calc}}$ / $\text{gcm}^{-3}$	1.340
$\mu$ / $\text{mm}^{-1}$	0.504
F(000)	1780.0
Crystal size / $\text{mm}^3$	$0.51 \times 0.17 \times 0.104$
Radiation	MoK $\alpha$ ( $\lambda = 0.71073$ )
2 $\theta$ Range for Data Collection / °	3.12 to 55.158
Index Ranges	$-16 \leq h \leq 14, -21 \leq k \leq 21, -24 \leq l \leq 28$
Reflections Collected	77631
Independent Reflections	20302 [ $R_{\text{int}} = 0.1023, R_{\text{sigma}} = 0.1197$ ]
Data / Restraints / Parameters	20302/1151/973
Goodness-of-fit on $F^2$	0.984
Final R indexes [ $ I  \geq 2\sigma(I)$ ]	$R_1 = 0.0758, wR_2 = 0.1894$
Final R indexes [all data]	$R_1 = 0.1158, wR_2 = 0.2114$
Largest diff. peak/hole / $\text{e} \text{Å}^{-3}$	1.16/-0.88
Flack Parameter	0.086(17)

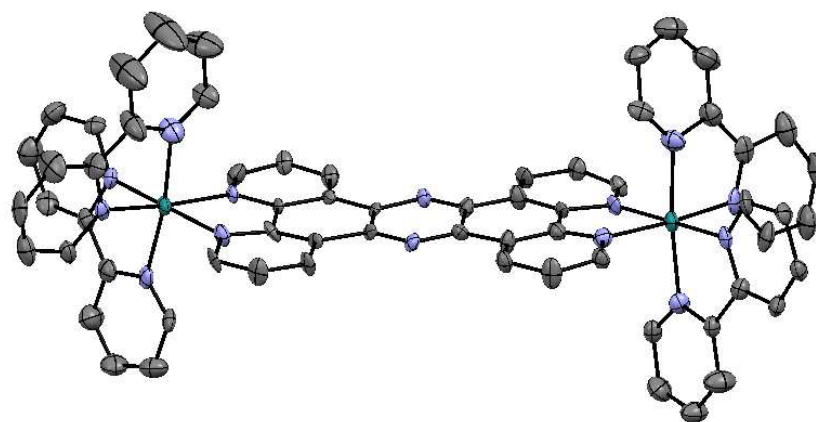


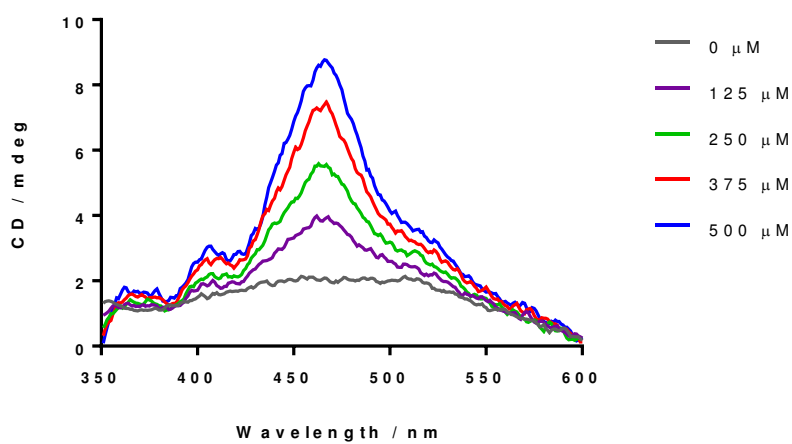
**Figure S3.** ORTEP plot of the X-ray crystallographic structure of  $\Delta,\Delta$ -1 with thermal ellipsoids indicating 50% probability. Counter ions and solvent molecules omitted for clarity.

X-ray quality crystals of the chloride salt of  $\Lambda,\Delta$ -**1** were grown using vapor diffusion of a concentrated solution of pure  $\Lambda,\Delta$ -**1** in methanol. Slow evaporation of the acetone antisolvent produced ruby red crystals suitable for structure determination. X-ray quality crystals of the hexafluorophosphate salts of  $\Lambda,\Lambda$ -**1** and  $\Delta,\Delta$ -**1** were grown using a similar vapor diffusion method from concentrated solution of pure  $\Lambda,\Lambda$ -**1** or  $\Delta,\Delta$ -**1** in nitromethane with diethyl ether as the antisolvent.

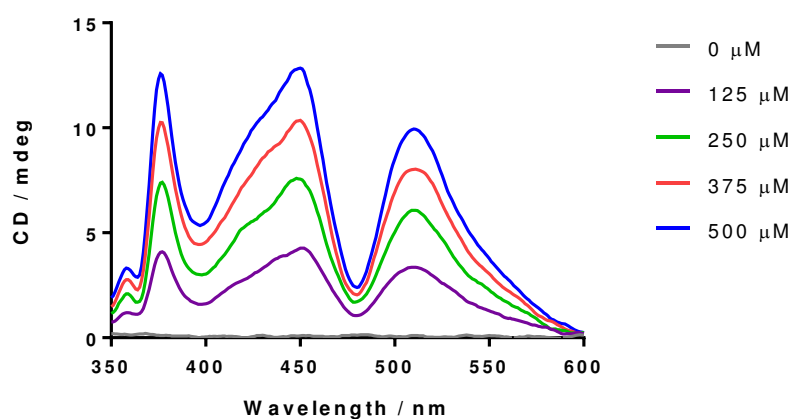
The intensity data was obtained on either a Bruker Kappa Apex-II CCD or Bruker Kappa Apex-II diffractometer operating with a MoK $\alpha$  sealed-tube X-ray source, or a Bruker D8 Venture diffractometer equipped with a Photon 100 CMOS detector using a CuK $\alpha$  microfocus X-ray source at 100 K. The reflections were corrected for absorption via empirical methods (SADABS) based upon symmetry-equivalent reflections combined with measurements at varied azimuthal angles.<sup>1,2</sup> The crystal structure was solved and refined against F<sup>2</sup> values using ShelXT for solution and ShelXL for refinement through the Olex2 program.<sup>2-5</sup> Non-hydrogen atoms were refined anisotropically and hydrogen atoms were placed in calculated geometries and refined utilizing a riding model and isotropic displacement parameters.

## SI 2

(a)  $\Lambda,\Delta$



(b)  $\Lambda,\Lambda$



(c)  $\Delta,\Delta$

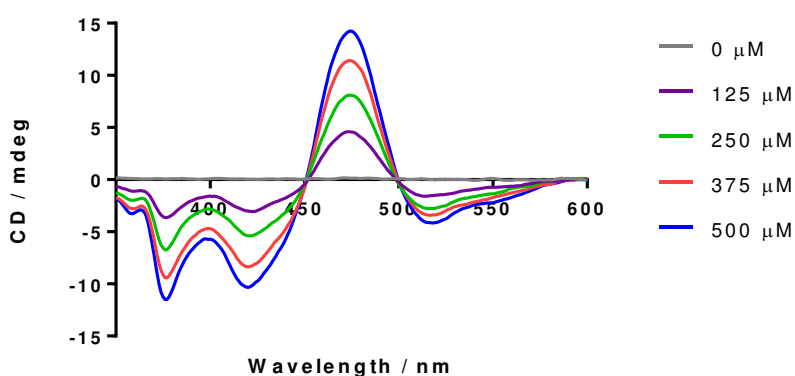


**Figure S4.** CD spectra of 2 mM d(GCATATCG).(CGATATGC) in 5 mM tris buffer at pH 7.4 with 150 mM NaCl, with addition of increasing concentrations of **1**. (a)  $\Lambda,\Delta$ -**1**. Control spectra of  $\Lambda,\Delta$ -**1** alone have no signal in this region. (b)  $\Lambda,\Lambda$ -**1**. Control spectra of  $\Lambda,\Lambda$ -**1** alone at these concentrations were subtracted to give these spectra. (c)  $\Delta,\Delta$ -**1**. Control spectra of  $\Delta,\Delta$ -**1** alone at these concentrations were subtracted to give these spectra.

### SI 3

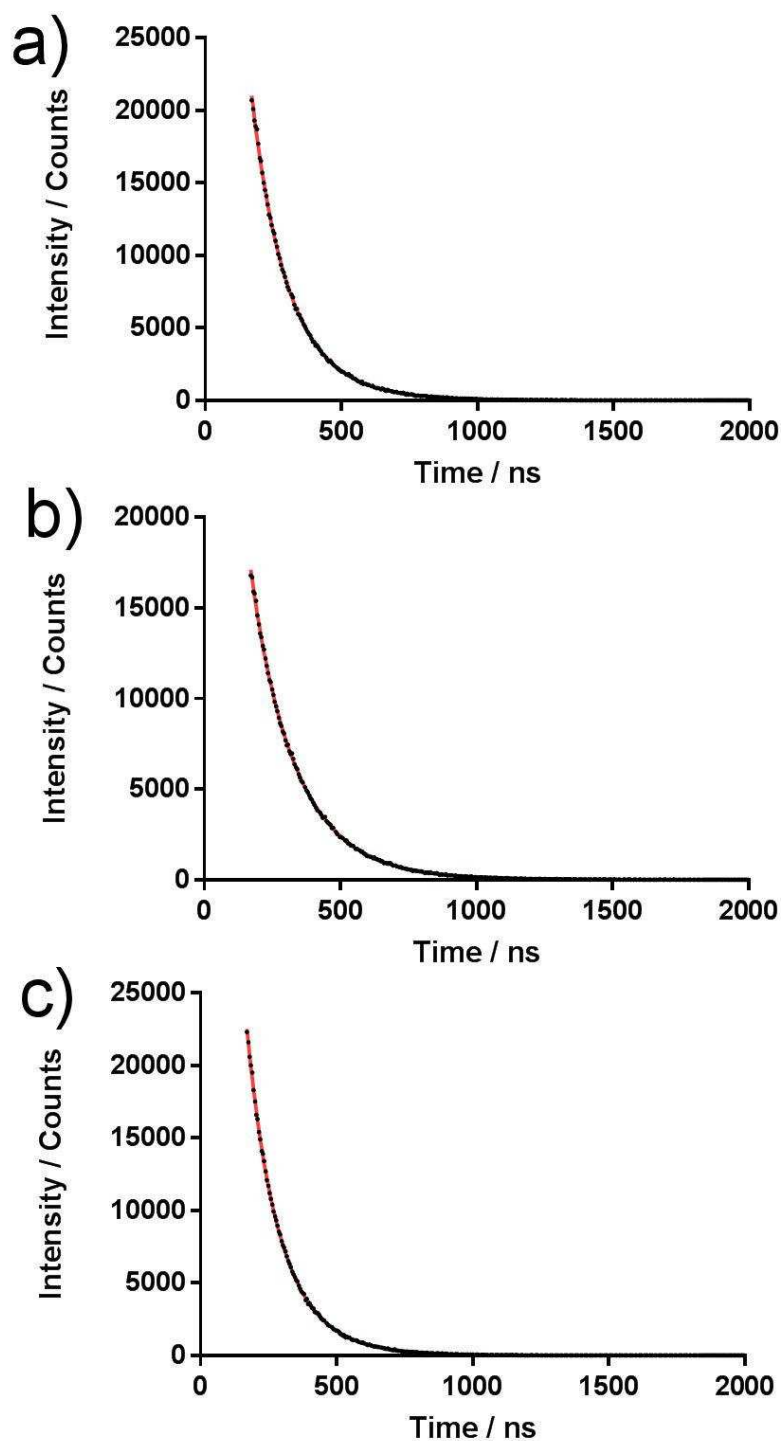


**Figure S5.** Luminescence lifetime decay spectra for 0.5 mM **1** and 2mM d(GCATATCG).d(CGATATCG). The data were fitted to a two-exponential decay function. (a)  $\Lambda, \Delta-1$ , fitted to  $\tau = 164.4 \pm 3.7$  ns with 71% population, and  $\tau = 99.4 \pm 5.5$  ns with 29% population. (b)  $\Lambda, \Lambda-1$ , fitted to  $\tau = 147.4 \pm 5.8$  ns with 69% population, and  $\tau = 90.5 \pm 6.5$  ns with 31% population. (c)  $\Delta, \Delta-1$ , fitted to  $\tau = 175.6 \pm 1.4$  ns with 95% population, and  $\tau = 72.0 \pm 10.7$  ns with 5% population.

## SI 4

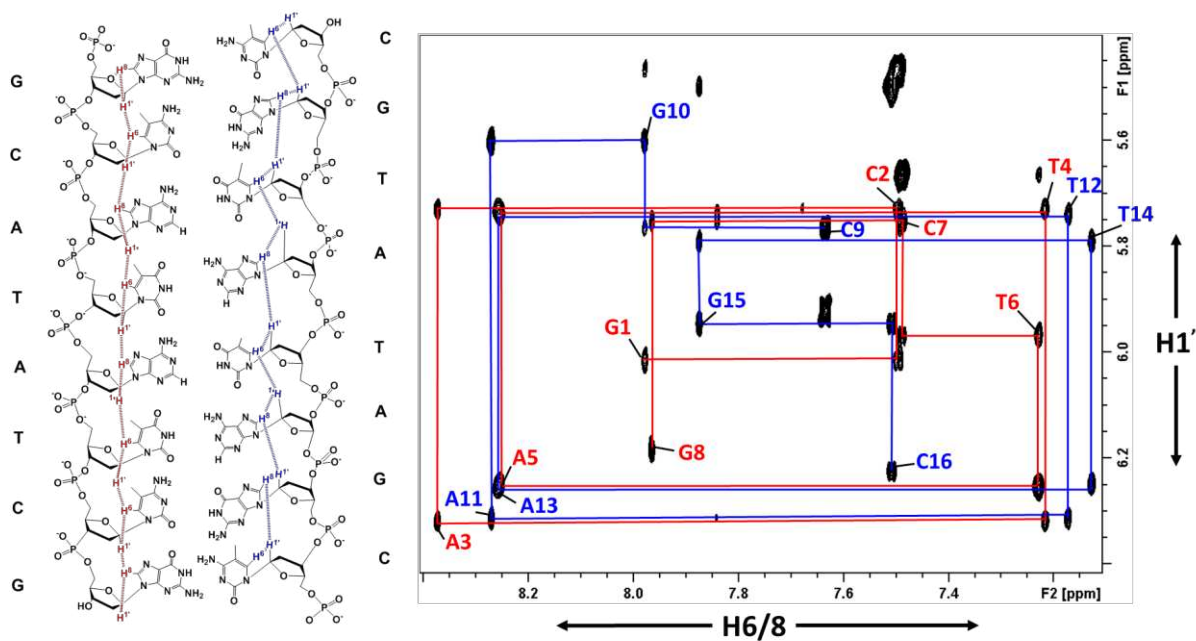


**Figure S6.** The H1'-H6/8 NOE walk for the free DNA duplex d(GCATATCG).d(CGTATAGC), 2 mM in D<sub>2</sub>O at 298K. All homonuclear NMR experiments were carried out on a Bruker Avance 800 MHz spectrometer. DNA samples were prepared in D<sub>2</sub>O with 25 mM NaCl. Oligonucleotide was used at 2 mM in order to ensure a completely duplex sample as melting of the strands occurred at lower concentrations. DNA assignments were made using standard TOCSY, COSY and NOESY experiments. Mixing times for the TOCSY and NOESY experiments were 60 ms and 200 ms respectively.

## SI 5

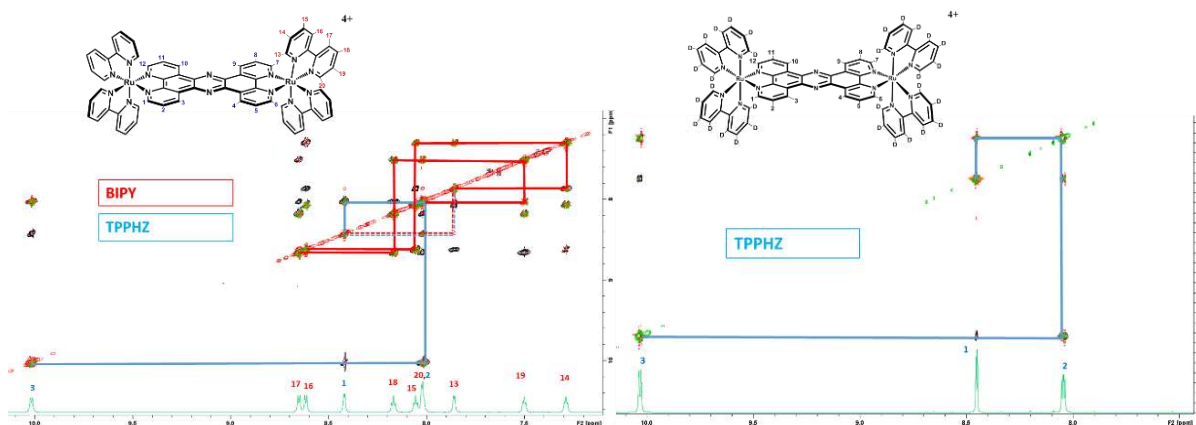


**Figure S7.** 2D NMR assignment of free metal complexes. Spectra are TOCSY (black), COSY (green) and NOESY (red). Blue and red lines correlate the spin systems of the tpphz and bipyridine respectively. The dashed red/blue indicates a bipyridine-tpphz inter-ligand NOE crosspeak.

## SI 6

**Table S1.** Full resonance assignment of DNA duplex d(GCATATCG).d(CGTATAGC) and changes in chemical shift upon addition of the optical isomers of  $[\{\text{Ru}(\text{bpy-d}_8)_2\}_2(\text{tpphz})]^{4+}$

	H8	H6	H5	H1'	H2'	H2''	H3'	me
<b>G1</b>	<b>7.98</b>	-	-	<b>6.01</b>	<b>2.64</b>	<b>2.82</b>	<b>4.87</b>	-
$\Lambda, \Lambda$ -1	-0.04	-	-	-0.04	0.01	-0.06	-0.05	-
$\Lambda, \Lambda$ -2	-0.17	-	-	-0.25	-0.15	-0.21	-0.04	-
$\Lambda, \Delta$	-0.04	-	-	-0.04	0.01	-0.06	-0.06	-
<b>C2</b>	-	<b>7.49</b>	<b>5.46</b>	<b>5.73</b>	<b>2.20</b>	<b>2.52</b>	<b>4.92</b>	-
$\Lambda, \Lambda$ -1	-	-0.04	-0.10	-0.03	-0.10	-0.13	0.02	-
$\Lambda, \Lambda$ -2	-	0.24	-0.25	0.38	0.60	-0.13	0.30	-
$\Lambda, \Delta$	-	-0.06	-0.15	0.01	-0.13	-0.12	-0.01	-
<b>A3</b>	<b>8.37</b>	-	-	<b>6.32</b>	<b>2.74</b>	<b>3.00</b>	<b>5.06</b>	-
$\Lambda, \Lambda$ -1	-0.40	-	-	-0.23	-0.42	-0.26	-0.11	-
$\Lambda, \Lambda$ -2	0.18	-	-	-0.56	0.14	-0.06	0.02	-
$\Lambda, \Delta$	-0.25	-	-	-0.17	-0.31	-0.18	-0.06	-
<b>T4</b>	-	<b>7.22</b>	-	<b>5.73</b>	<b>2.16</b>	<b>2.54</b>	<b>4.92</b>	<b>1.53</b>
$\Lambda, \Lambda$ -1	-	-0.15	-	-0.19	0.33	-0.12	0.14	-1.61
$\Lambda, \Lambda$ -2	-	-0.02	-	0.01	-0.05	0.02	-0.02	-0.18
$\Lambda, \Delta$	-	-0.02	-	-0.11	0.39	0.01	0.19	-0.96
<b>A5</b>	<b>8.26</b>	-	-	<b>6.25</b>	<b>2.67</b>	<b>2.93</b>	<b>5.01</b>	-
$\Lambda, \Lambda$ -1	0.27	-	-	-0.57	0.05	-0.09	-0.10	-
$\Lambda, \Lambda$ -2	0.04	-	-	0.02	0.01	-0.01	0.01	-
$\Lambda, \Delta$	0.18	-	-	-0.59	-0.04	-0.17	-0.17	-
<b>T6</b>	-	<b>7.23</b>	-	<b>5.97</b>	<b>2.03</b>	<b>2.45</b>	<b>4.87</b>	<b>1.35</b>

$\Lambda, \Lambda-1$	-	-0.12	-	-0.11	-0.07	-0.03	-0.02	-0.13
$\Lambda, \Lambda-2$	-	-0.01	-	-0.09	-0.01	-0.04	-0.02	0.08
$\Lambda, \Delta$	-	-0.18	-	-0.24	-0.05	-0.09	-0.02	-0.23
<b>C7</b>	-	<b>7.49</b>	<b>5.67</b>	<b>5.75</b>	<b>2.02</b>	<b>2.38</b>	<b>4.86</b>	-
$\Lambda, \Lambda-1$	-	0.01	-0.01	-0.06	0.01	0.01	-0.01	-
$\Lambda, \Lambda-2$	-	-0.02	-0.01	-0.04	-0.02	0.00	-0.02	-
$\Lambda, \Delta$	-	0.00	-0.04	0.00	-0.03	-0.02	0.01	-
<b>G8</b>	<b>7.96</b>	-	-	<b>6.18</b>	<b>2.63</b>	<b>2.38</b>	<b>4.69</b>	-
$\Lambda, \Lambda-1$	-0.01	-	-	-0.03	-0.01	-0.02	-0.02	-
$\Lambda, \Lambda-2$	-0.02	-	-	-0.02	-0.02	-0.02	-0.01	-
$\Lambda, \Delta$	-0.02	-	-	-0.04	-0.03	-0.02	-0.01	-
<b>C9</b>	-	<b>7.64</b>	<b>5.92</b>	<b>5.76</b>	<b>1.92</b>	<b>2.41</b>	<b>4.71</b>	-
$\Lambda, \Lambda-1$	-	-0.02	-0.07	-0.04	0.03	-0.02	-0.01	-
$\Lambda, \Lambda-2$	-	0.00	-0.06	-0.03	0.06	-0.01	-0.01	-
$\Lambda, \Delta$	-	0.01	-0.05	-0.03	0.09	0.02	-0.01	-
<b>G10</b>	<b>7.98</b>	-	-	<b>5.60</b>	<b>2.76</b>	<b>2.85</b>	<b>5.03</b>	-
$\Lambda, \Lambda-1$	-0.02	-	-	-0.09	-0.01	-0.06	0.00	-
$\Lambda, \Lambda-2$	-0.02	-	-	-0.01	-0.02	-0.02	-0.01	-
$\Lambda, \Delta$	-0.03	-	-	0.05	-0.04	-0.01	-0.01	-
<b>A11</b>	<b>8.27</b>	-	-	<b>6.31</b>	<b>2.70</b>	<b>3.00</b>	<b>5.06</b>	-
$\Lambda, \Lambda-1$	-0.35	-	-	-0.20	-0.37	-0.27	-0.07	-
$\Lambda, \Lambda-2$	-0.05	-	-	-0.02	0.02	-0.03	-0.04	-
$\Lambda, \Delta$	-0.17	-	-	-0.13	-0.21	-0.10	-0.01	-
<b>T12</b>	-	<b>7.17</b>	-	<b>5.74</b>	<b>2.12</b>	<b>2.54</b>	<b>4.89</b>	<b>1.47</b>
$\Lambda, \Lambda-1$	-	-0.07	-	-0.18	0.37	-0.19	0.17	-1.35
$\Lambda, \Lambda-2$	-	-0.04	-	-0.05	-0.08	-0.19	0.03	-0.10
$\Lambda, \Delta$	-	0.17	-	-0.02	0.53	-0.14	0.25	-0.49
<b>A13</b>	<b>8.26</b>	-	-	<b>6.25</b>	<b>2.63</b>	<b>2.93</b>	<b>5.02</b>	-
$\Lambda, \Lambda-1$	0.25	-	-	-0.61	0.10	-0.11	-0.09	-
$\Lambda, \Lambda-2$	-0.54	-	-	-0.27	-0.63	-0.43	-0.02	-
$\Lambda, \Delta$	0.21	-	-	-0.58	0.12	-0.12	-0.06	-
<b>T14</b>		<b>7.13</b>	-	<b>5.79</b>	<b>1.99</b>	<b>2.40</b>	<b>4.89</b>	<b>1.37</b>
$\Lambda, \Lambda-1$	-	-0.06	-	-0.15	-0.10	-0.04	-0.04	-0.12
$\Lambda, \Lambda-2$	-	-0.33	-	-0.29	0.36	0.17	0.10	-2.17
$\Lambda, \Delta$	-	-0.05	-	-0.14	-0.03	-0.03	-0.01	-0.15
<b>G15</b>	<b>7.87</b>	-	-	<b>5.94</b>	<b>2.64</b>	<b>2.75</b>	<b>4.98</b>	-
$\Lambda, \Lambda-1$	0.03	-	-	0.02	0.02	-0.01	0.01	-
$\Lambda, \Lambda-2$	0.08	-	-	-0.61	-0.06	-0.11	-0.27	-
$\Lambda, \Delta$	0.03	-	-	0.05	0.01	0.00	0.02	-
<b>C16</b>	-	<b>7.50</b>	<b>5.50</b>	<b>6.22</b>	<b>2.19</b>	<b>2.19</b>	<b>4.51</b>	-
$\Lambda, \Lambda-1$	-	-0.02	0.01	-0.04	-0.02	-0.02	-0.01	-
$\Lambda, \Lambda-2$	-	-0.27	-0.27	-0.41	-0.23	-0.12	-0.11	-
$\Lambda, \Delta$	-	-0.03	-0.02	-0.05	0.00	0.00	0.00	-

## SI 7

**Table S2.** Changes in ruthenium complex chemical shift upon DNA binding

$\Lambda, \Lambda$ -1a	1	2	3	4	5	6	7	8	9	10	11	12
$\delta/\text{ppm}$	8.16	7.07	8.31	9.18	7.95	8.38	8.38	7.96	9.09	8.35	7.33	8.27
$\Delta\delta$	-0.30	-0.98	-1.72	-0.85	-0.10	-0.08	-0.07	-0.09	-0.94	-1.68	-0.72	-0.19
$\Lambda, \Lambda$ -1b	1	2	3	4	5	6	7	8	9	10	11	12
$\delta/\text{ppm}$	8.38	8.00	9.02	8.44	7.77	8.23	8.42	7.81	9.09	8.26	6.67	8.10
$\Delta\delta$	-0.08	-0.05	-1.01	-1.59	-0.28	-0.22	-0.04	-0.24	-0.94	-1.77	-1.38	-0.36
$\Delta, \Lambda$ -1	1	2	3	4	5	6	7	8	9	10	11	12
$\delta/\text{ppm}$	8.22	6.96	8.43	9.05	7.88	8.33	8.42	7.90	8.81	8.57	7.54	8.44
$\Delta\delta$	-0.24	-1.09	-1.61	-0.98	-0.17	-0.13	-0.04	-0.15	-1.23	-1.46	-0.51	-0.02

## SI 8

**Table S3.** Intermolecular NOEs between DNA duplex d(GCATATCG). d(CGTATAGC) and the optical isomers of  $[\{\text{Ru}(\text{bpy-d}_8)_2\}_2(\text{tpphz})]^{4+}$

$\Lambda, \Lambda$ -1a	H1	H2	H3	H4	H5	H6	H7	H8	H9	H10	H11	H12
T4							Me	Me	Me,2',2"	1',2',2"	1',2',2"	1',2',2"
A5										1'	1'	1'
T12	1'	1'	1',2',2"	Me,2',2"	Me	Me						
A13	1'	1'	1'									
$\Lambda, \Lambda$ -1b	H1	H2	H3	H4	H5	H6	H7	H8	H9	H10	H11	H12
C2							H5	H5	H5,1'	1',2',2"	1',2',2"	1'
A3										1'	1'	1'
T14			1',2',2"	Me,2',2"	Me	Me						

G15      1'      1'

$\Lambda, \Delta$ -1a	H1	H2	H3	H4	H5	H6	H7	H8	H9	H10	H11	H12
T4							Me	Me	Me,2',2''	1',2',2''	1',2',2''	2''
A5												
T12		1',2',2''	1',2',2''	Me,2'	Me	Me						
A13	1'		1'									

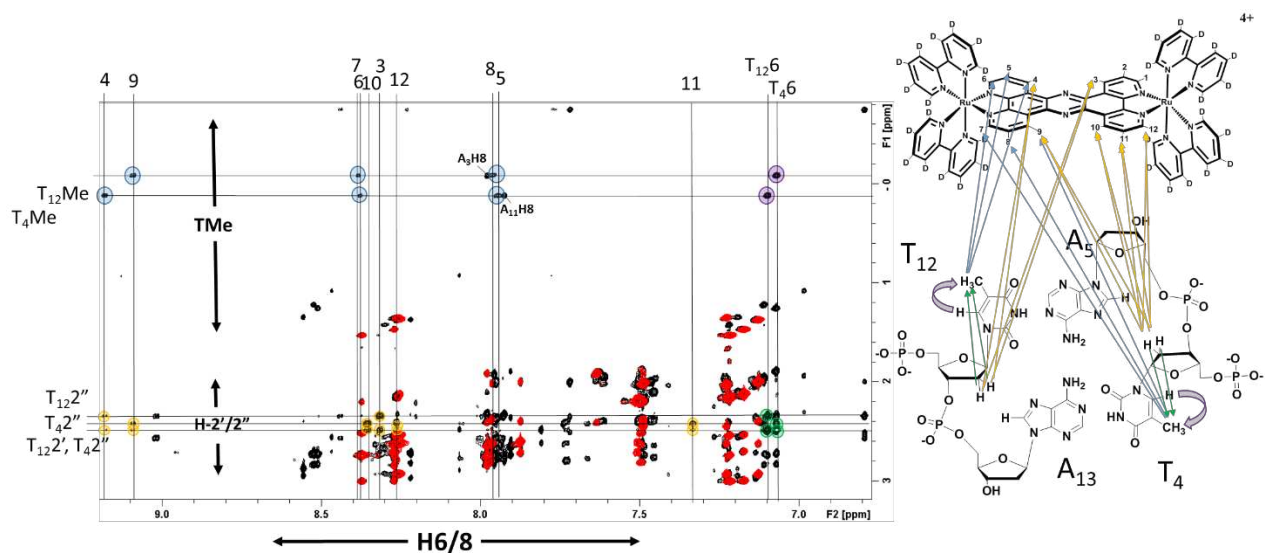


**Figure S8.** Intermolecular NOEs involving d- $\Lambda, \Lambda$ -1A. An expansion of the 2',2'' and TMe-aromatic region of the NOESY spectrum of d(GCATATCG).d(CGTAGTAGC) (red), overlaid onto a spectrum containing half an equivalent of d- $\Lambda, \Lambda$ -1 (black). The intramolecular NOE correlations H6/2',2'' (green) and H6/TMe (purple) and the intermolecular NOE correlations d- $\Lambda, \Lambda$ -1A/TMe (blue) and d- $\Lambda, \Lambda$ -1A/H2',2'' (orange) are located in both grooves of the DNA. A schematic of the (T<sub>4</sub>,A<sub>13</sub>)|(T<sub>12</sub>,A<sub>5</sub>) binding site is given for reference.

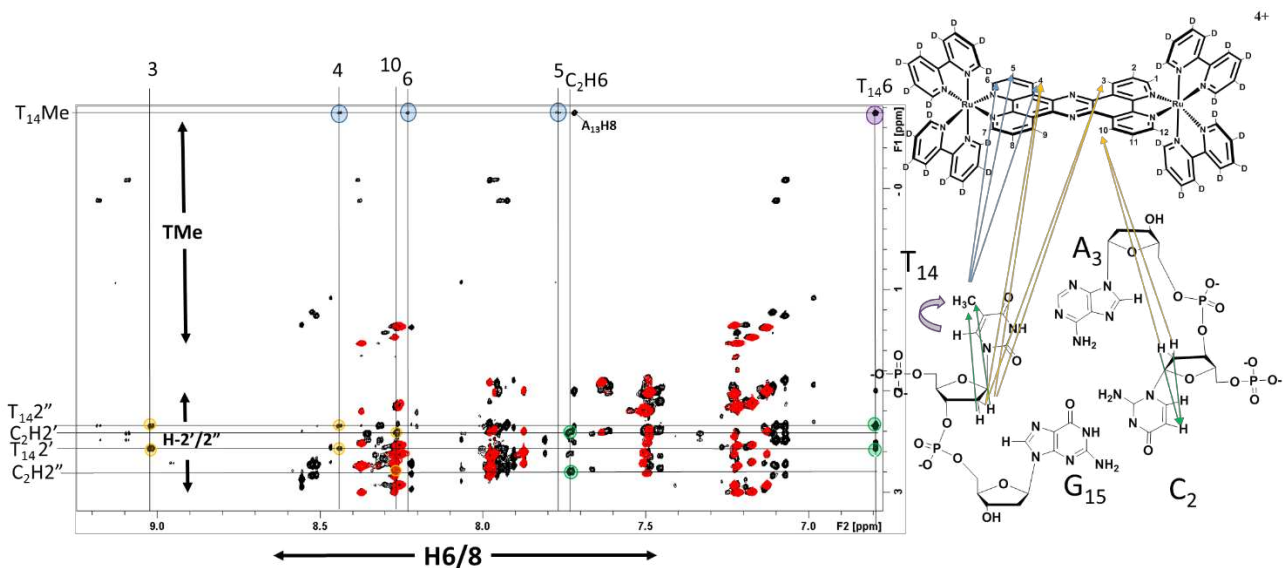


**Figure S9.** Intermolecular NOEs involving d- $\Delta,\Delta$ -1B. An expansion of the 2',2'' and TMe-aromatic region of the NOESY spectrum of d(GCATATCG).(CGTAGTAGC) (red), overlaid onto a spectrum containing half an equivalent of  $\Delta,\Delta$ -1 (black). The intermolecular NOE correlations H6/2',2'' (green) and H6/TMe (purple) and the intramolecular NOE correlations d- $\Delta,\Delta$ -1B/TMe (blue) and d- $\Delta,\Delta$ -1B/H2',2'' (yellow) are located in both grooves of the DNA. A schematic of the (T<sub>4</sub>,A<sub>13</sub>)|(T<sub>12</sub>,A<sub>5</sub>) binding site is given for reference.

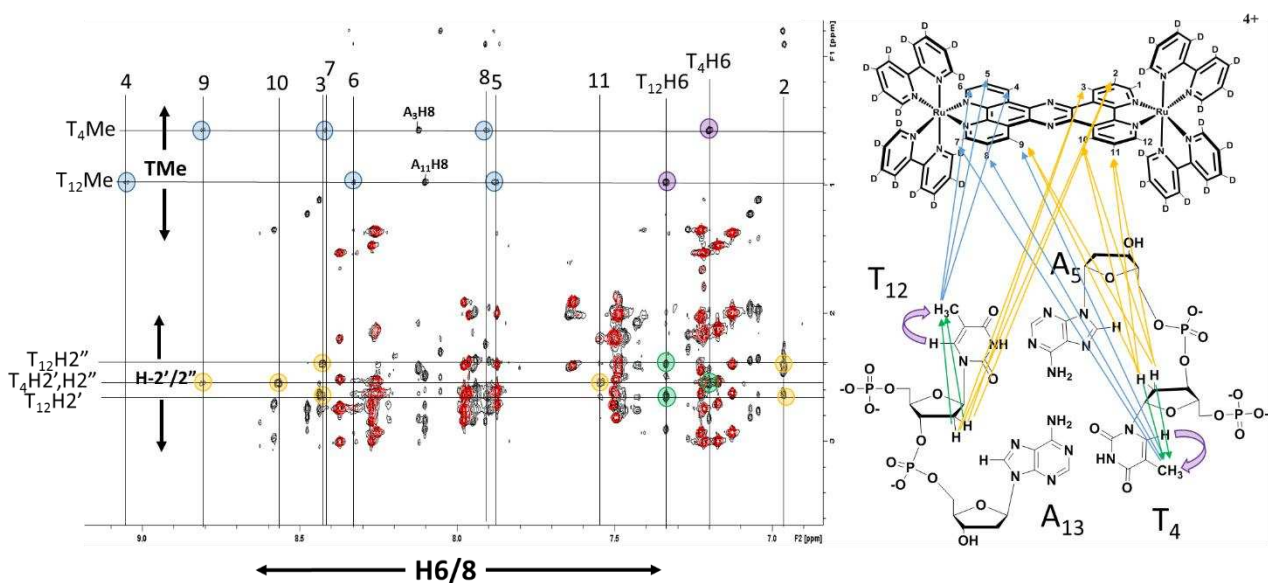


**Figure S10.** Intermolecular NOEs involving d- $\Delta,\Delta$ -1A. Expansion of the 2',2'' and TMe-aromatic region of the NOESY spectrum of a 2 mM D<sub>2</sub>O solution containing d(GCATATCG).d(CGTAGTAGC) (red), overlaid onto a spectrum containing half an equivalent of d- $\Delta,\Delta$ -1 (black), indicating the intermolecular NOE correlations H6/2',2'' (green) and H6/TMe (purple) and the intramolecular NOE correlations d- $\Delta,\Delta$ -1A/TMe (blue) and d- $\Delta,\Delta$ -1A/H2',2'' (orange) located in both grooves of the DNA. A schematic of the (T<sub>4</sub>,A<sub>13</sub>)|(T<sub>12</sub>,A<sub>5</sub>) binding site is given for reference.

## SI 9

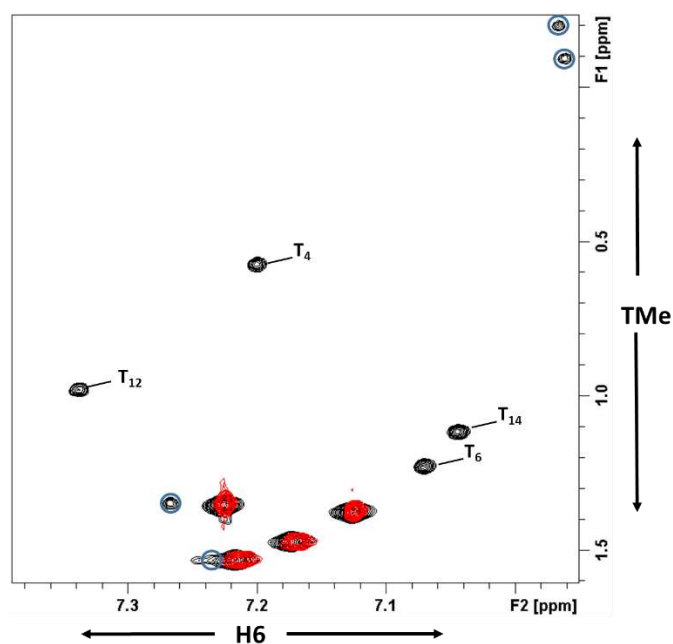


**Figure S11.** Expansion of the H6-TMe region of the TOCSY spectrum of a 2 mM D<sub>2</sub>O solution containing duplex sequence d(GCATATCG).d(CGTAGTAGC) (red), overlaid onto a spectrum containing half an equivalent of  $\Lambda$ , $\Delta$ -**1** (black). The H6-TMe cross peaks for the d- $\Lambda$ , $\Delta$ -**1A** are indicated, and the blue circles indicate the d- $\Lambda$ , $\Delta$ -**1B** H6-TMe cross peaks.

## SI 10

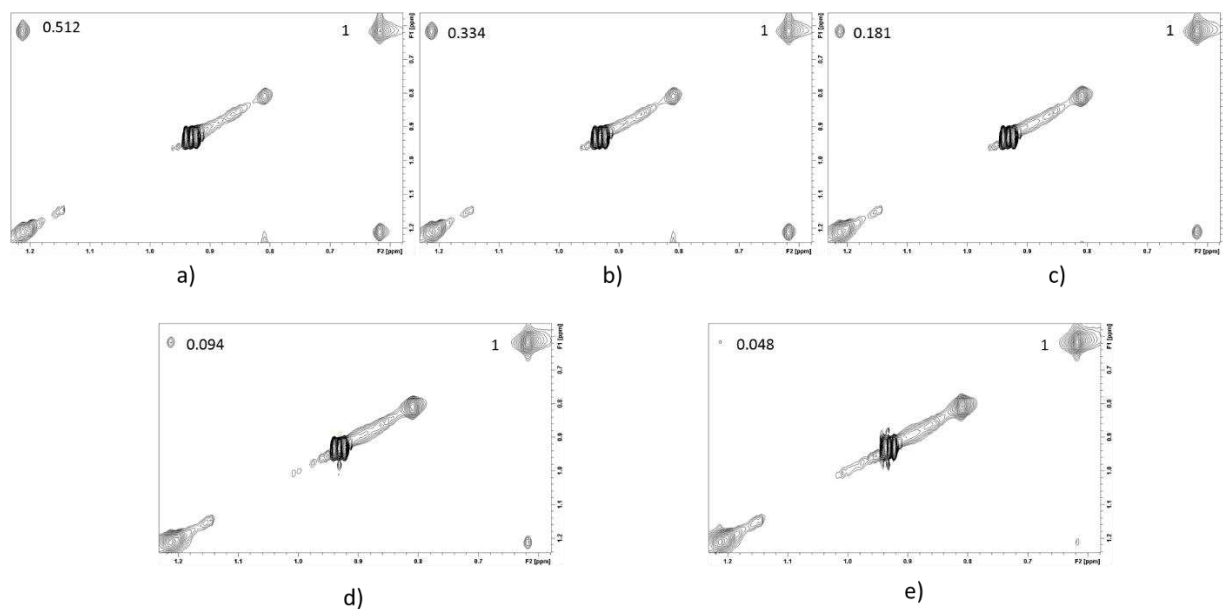


**Figure S12.** EXSY NMR experiment from the thymidine methyl region of the NOESY spectrum of the d- $\Delta$ , $\Delta$ -**1**/DNA complex at 298 K showing cross peak and diagonal peak intensities of the two exchanging conformations of d- $\Delta$ , $\Delta$ -**1** using mixing times of a) 1 s b) 500 ms c) 200 ms d) 100 ms and e) 50 ms.

The ratio of cross peak intensity  $I_x$  to diagonal peak intensity  $I_d$  ( $I_x/I_d$ ) at several mixing times ( $t_m$ ) can be used to derive an equilibrium rate constant  $k_r$ . The  $k_r$  can be derived by fitting to the equation  $I_x/I_d = \left[ \frac{1 - e^{-k_r t_m}}{1 + e^{-k_r t_m}} \right]^6$ . EXSY experiments were carried out with mixing times of 50, 100, 200, 500 and 1000 ms (and 2 s at 293 and 303 K), at temperatures of 288, 293, 298, 303 and 308 K, and the data were fitted using Sigmaplot®.

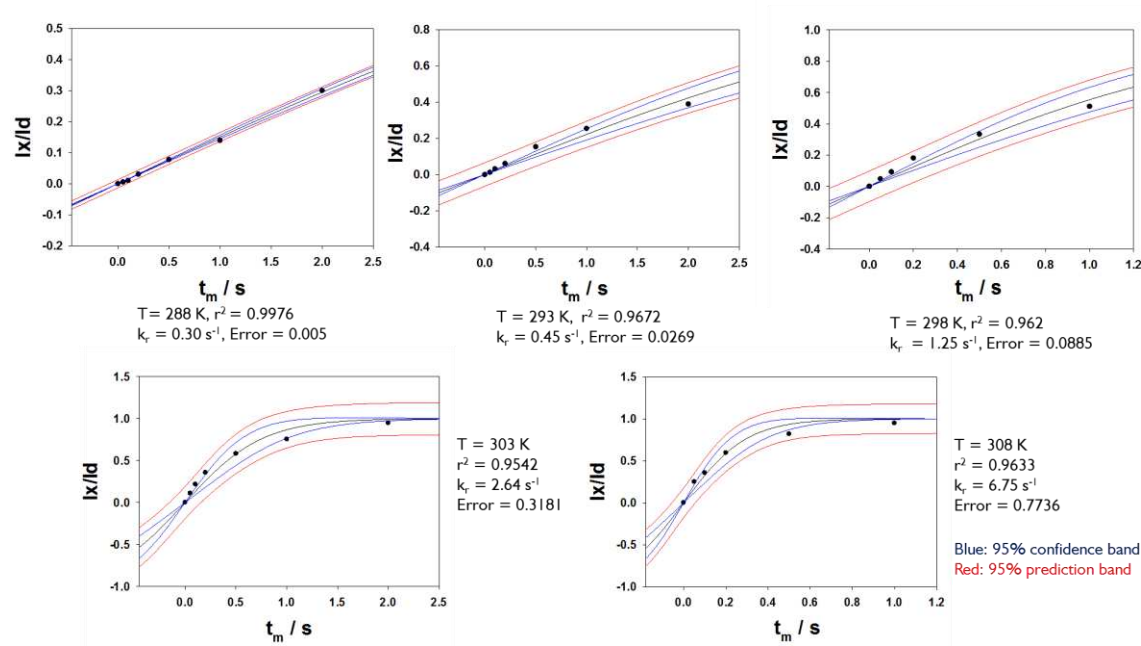


**Figure S13.** d- $\Delta$ -1/DNA EXSY build up data giving ( $I_x/I_d$ ) at different mixing times ( $t_m$ ) (50, 100, 200, 500, 1000, 2000 ms) and temperatures a) 288 K, b) 293 K, c) 298 K, d) 303 K and e) 308 K fitted to equation above. 95% confidence bands are shown in blue and 95% prediction bands are shown in red.

The Arrhenius equation is  $k_r = A \cdot e^{-\frac{E_a}{RT}}$  where  $E_a$  is the activation energy,  $R$  is the gas constant,  $T$  is temperature and  $A$  is the Arrhenius frequency factor.  $E_a$  can be derived by fitting the temperature dependency of the rate constants using the equation  $\ln(k_r) = \ln(A) - \frac{E_a}{RT}$

The Eyring equation is  $k_r = K \frac{k_b T}{h} e^{-\frac{\Delta G^\ddagger}{RT}}$ . Assuming a transmission coefficient ( $K$ ) of 1, an Eyring plot can give enthalpy and entropy terms by fitting to the equation  $\ln\left(\frac{k_r}{T}\right) = \ln\left(\frac{k_b}{h}\right) - \frac{\Delta H^\ddagger}{RT} + \frac{\Delta S^\ddagger}{R}$

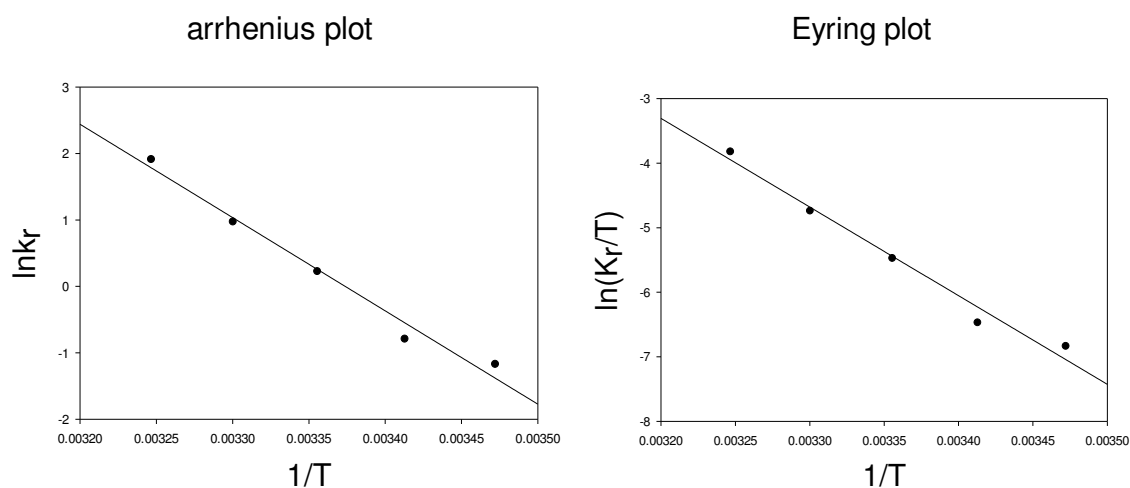


**Figure S14.** Linear Arrhenius plot and Eyring plots produced from exchange rate constants for the  $\Delta,\Delta$  DNA complex at varied temperatures, giving  $E_a = 116.7 \text{ kJmol}^{-1}$ ,  $\Delta H^\ddagger = 114.1 \text{ kJmol}^{-1}$  and  $\Delta S^\ddagger = 140.3 \text{ Jmol}^{-1}\text{K}^{-1}$ .

### SI 11

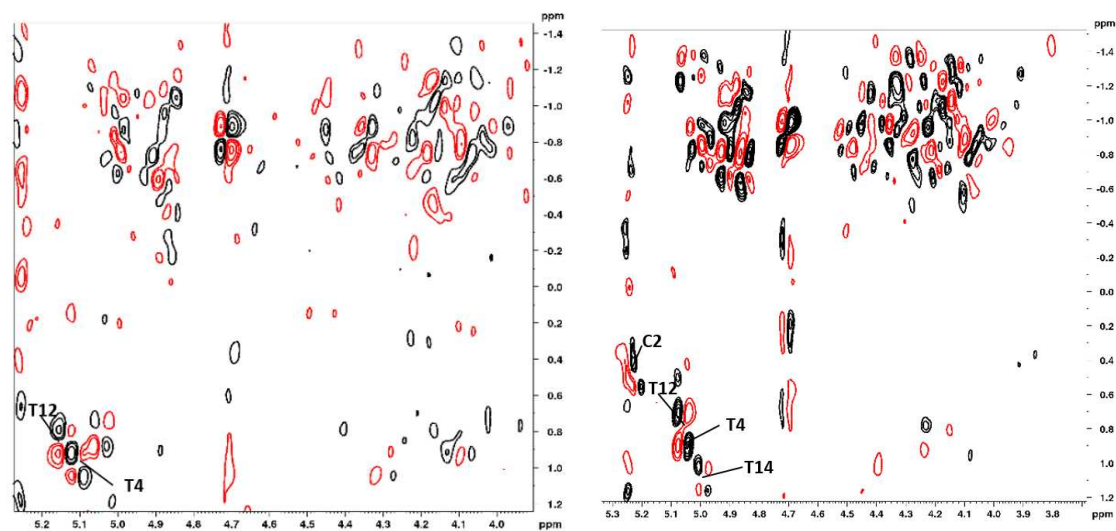


**Figure S15.**  $^1\text{H}$ - $^{31}\text{P}$  COSY of 2 mM DNA oligo containing 1 mM d- $\Lambda,\Delta$ -1 (left) and 1 mM d- $\Lambda,\Lambda$ -1 (right). The highly shifted  $3\text{H}'$ - $^{31}\text{P}$  peaks are labelled, where F1 is  $^1\text{H}$  and F2 is  $^{31}\text{P}$ . All  $^{31}\text{P}$  and  $^{31}\text{P}$ - $^1\text{H}$  COSY experiments were carried out on a Bruker Avance 500 MHz spectrometer.

## SI 12

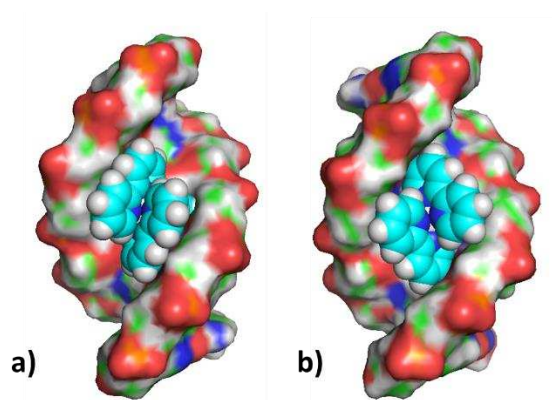


**Figure S16.** Views from the minor groove of the two conformations of the  $\Lambda, \Delta$ -1: d(GCATATCG).d(CGATATGC) complex with a)  $\Lambda$  in the minor groove and b)  $\Delta$  in the minor groove.

### References

- (1) Bruker. *SADABS*; Bruker Axs Inc.: Madison, Wisconsin, USA, 2016.
- (2) Krause, L.; Herbst-Irmer, R.; Sheldrick, G. M.; Stalke, D. Comparison of silver and molybdenum microfocus X-Ray sources for single-crystal structure determination. *J. Appl. Crystallogr.* **2015**, *48* (1), 3–10. <https://doi.org/10.1107/S1600576714022985>.
- (3) Sheldrick, G. M. SHELXT - Integrated space-group and crystal-structure determination. *Acta Crystallogr. Sect. A Found. Crystallogr.* **2015**, *71* (1), 3–8. <https://doi.org/10.1107/S2053273314026370>.
- (4) Sheldrick, G. M. Crystal structure refinement with SHELXL. *Acta Crystallogr. Sect. C Struct. Chem.* **2015**, *71* (1), 3–8. <https://doi.org/10.1107/S2053229614024218>.
- (5) Dolomanov, O. V.; Bourhis, L. J.; Gildea, R. J.; Howard, J. A. K.; Puschmann, H. OLEX2: A Complete structure solution, refinement and analysis program. *J. Appl. Crystallogr.* **2009**, *42* (2), 339–341. <https://doi.org/10.1107/S0021889808042726>.
- (6) Bodenhausen, G.; Ernst, R. R. Direct determination of rate constants of slow dynamic processes by two-dimensional Accordion spectroscopy in NMR. *J. Am. Chem. Soc.* **1982**, *104* (5), 1304.